

# Long-term impact of temperature on the hydraulic permeability of bentonite

J. F. HARRINGTON<sup>1</sup>\*, G. VOLCKAERT<sup>2</sup> & D. J. NOY<sup>1</sup>

<sup>1</sup>*Transport Properties Research Laboratory, British Geological Survey, Keyworth, Nottingham NG12 5GG, UK*

<sup>2</sup>*Studiecentrum voor Kernenergie (SCK-CEN), Boeretang 200, 2400 Mol, Belgium*

\*Corresponding author (e-mail: [jfha@bgs.ac.uk](mailto:jfha@bgs.ac.uk))

**Abstract:** In a Swedish repository for the disposal of heat-emitting waste, the long-term thermal stability of the bentonite engineered barrier forms a key component of the safety case. Central to such consideration is the evolution of hydraulic permeability and a potential degradation of hydraulic properties, in response to prolonged thermal exposure of the clay. To address this issue, a detailed programme of laboratory-based experiments has been undertaken at both the British Geological Survey and Studiecentrum voor Kernenergie/Centre d'Etude de L'Energie Nucleaire, in order to examine the hydraulic behaviour of bentonite that had previously been exposed to elevated temperatures. Hydraulic properties were calculated from both steady-state pressure gradients and from analysis of the pressure transients. Inspection of the data found no significant difference in hydraulic behaviour between the virgin material and clay samples taken from the Canister Retrieval Test. Based on these observations, the authors find no evidence for an adverse increase in hydraulic conductivity of bentonite as a result of prolonged thermal exposure to temperatures of 80 °C.



**Gold Open Access:** This article is published under the terms of the CC-BY 3.0 license.

The thermal alteration of clay minerals resulting in the transition of smectite to illite is a well-established phenomenon and has been empirically observed by numerous researchers in the past (e.g. Velde *et al.* 1986; Bruce *et al.* 1987; Freed & Peacor 1989; Velde & Vasseur 1992; Lanson *et al.* 2009; Mosser-Ruck *et al.* 2010). A review of thermal stability of bentonite is given by Meunier *et al.* (1998). If such a reaction were to occur in a repository for heat-emitting waste, this thermally driven alteration and restructuring of the clay lattice to a lower swelling form of clay mineral would have a profound impact on the hydromechanical and geochemical properties of the resultant material. There is no single thermal activation energy for such reactions to occur, as these processes are highly dependent on the geochemistry of the system (e.g. Mosser-Ruck *et al.* 2010). However, recent work by Pusch *et al.* (2010) suggests that early-onset hydraulic degradation (i.e. an increase in hydraulic permeability) can occur in compact bentonite subject to prolonged temperatures of only 80 °C. While the experimental detail underpinning these observations is unclear, the authors report a two order of magnitude increase in permeability for two clay samples taken from the Canister Retrieval Test (CRT) test performed at the Äspö underground research laboratory. If correct, such an increase in permeability would

represent a major alteration of the smectite component in the bentonite and would compromise repository safety performance.

However, this work is in direct contradiction to earlier results presented by Pusch (1985), who, after examining bentonite samples from the buffer mass test (BMT) performed at Stripa in the early 1980s, reported no significant changes in permeability and concluded that 'the influence of heating was insignificant and that the important physical properties, swelling and permeability, were not altered'. While temperatures in the BMT were higher than those reported in the CRT (i.e. 125 v. 80 °C, respectively), the test was of much shorter duration (i.e. 1 year as opposed to 5 years for the CRT). Villar & Gómez-Espina (2009) performed a series of hydraulic tests on Febex bentonite compacted to a range of dry densities from 1.5 to 1.7 m<sup>3</sup> mg<sup>-1</sup>. While no consistent results were obtained, permeability was seen to increase with temperature. However, while the increase in permeability could not solely be explained by changes in viscosity, the magnitude of permeability increase was an order of magnitude less than that report by Pusch & Weston (2012), and no consistent behaviour was observed.

To investigate this issue, an independent programme of laboratory-based experiments was undertaken in parallel at the British Geological

Survey (BGS) and Studiecentrum voor Kernenergie (SCK-CEN), to examine the hydraulic behaviour of bentonite exposed to elevated temperatures. To prevent bias and to ensure impartiality, the studies were conducted in isolation. Complementary approaches were adopted by each institute (described below) to measure hydraulic permeability under a range of test conditions. In an attempt to replicate the experiments of Pusch *et al.* (2010), preserved test material was taken from a number of locations within the same CRT experiment. In addition, a control sample of 'virgin' bentonite, supplied by Clay Technology AB, was examined to define the hydraulic properties of unaltered material without thermal loading.

To minimize perturbation of the clay during testing, the BGS opted to perform a series of long-term controlled flow-rate experiments in which the magnitude of the hydraulic gradient imposed across each sample is a dependent variable, simply related to the volumetric flow rate. In these tests, head gradient is allowed to slowly evolve in response to the imposed flow rate. As such, if hydraulic permeability had increased owing to thermal degradation of the buffer, then the differential pressure for a given flow rate would scale accordingly, resulting in proportionately smaller differential pressures. Ascending and descending flow cycles were imposed across each sample to examine any underlying hysteresis while the specimen was subject to a fixed backpressure.

At the same time, a complimentary programme of constant pressure tests was performed at SCK-CEN. In these experiments flux in and out of the sample was carefully controlled by two high-precision syringe pumps, in order to accurately measure hydraulic behaviour under steady-state conditions. As part of the test programme experiments were performed for different durations to examine the impact of calculating permeability under non-equilibrium conditions during the transient phase of testing. An attempt was also made to measure the hydraulic conductivity using a much smaller gradient, that is, a 1 m water column to investigate what effect, if any, this may have on permeability.

## Data reduction

Data were transferred to a spread sheet for processing and plotting. Hydraulic transients were very well-defined and largely free of experimental noise.

The one-dimensional equation of flow is

$$S_s \frac{\partial h}{\partial t} = K \frac{\partial^2 h}{\partial x^2} \quad (1)$$

where  $S_s$  ( $\text{m}^{-1}$ ) is the specific storage,  $K$  ( $\text{m s}^{-1}$ ) is the hydraulic conductivity,  $h$  (m) is the hydraulic head and  $x$  (m) is distance in the flow direction. This equation must be solved subject to the boundary conditions:

$$q = \frac{Q}{A_s} = -K \left. \frac{\partial h}{\partial x} \right|_{x=0} \quad (2)$$

and

$$h = 0 \quad \text{at } x = L_s \quad (3)$$

where  $q$  ( $\text{m s}^{-1}$ ) is the Darcy velocity,  $Q$  ( $\text{m}^3 \text{s}^{-1}$ ) is the volumetric flow rate,  $A_s$  ( $\text{m}^2$ ) and  $L_s$  (m) are the cross-sectional area and length of the specimen, respectively. Hydraulic head is related to the pore pressure,  $P$  (Pa), by

$$h = \frac{P}{\rho_w g} \quad (4)$$

where  $\rho_w$  ( $\text{kg m}^{-3}$ ) is the density of water and  $g$  ( $=9.81 \text{ m s}^{-2}$ ) is the acceleration due to gravity.

The head at  $x = 0$  and flow at  $x = L_s$  as functions of time were obtained by numerically inverting the Laplace transform solution given in Appendix 1. Five parameters are required to define the solution. Three are experimentally determined:  $Q$ ,  $A_s$  and  $L_s$ . The remaining two are the material properties that the test is designed to determine (i.e.  $K$  and  $S_s$ ). In order to estimate the values of these parameters, a general nonlinear least squares fitting routine was used to minimize the differences between the calculated curves and the measured head data.

Hydraulic conductivity was also calculated from the head gradient at steady state, enabling the two values to be compared. Permeability,  $k$  ( $\text{m}^2$ ),

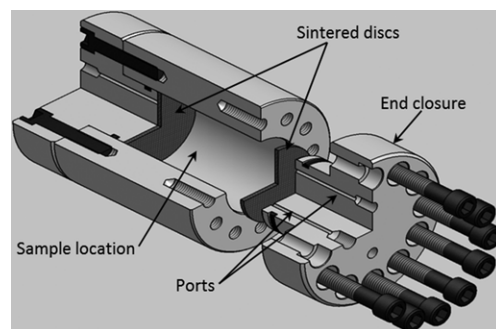


**Fig. 1.** Cut-through isometric diagram of the test vessel showing the location of the injection and backpressure ports, position of sintered filters and location of cap screws. One end-closure is shown removed from the bore of the vessel to illustrate individual system components.

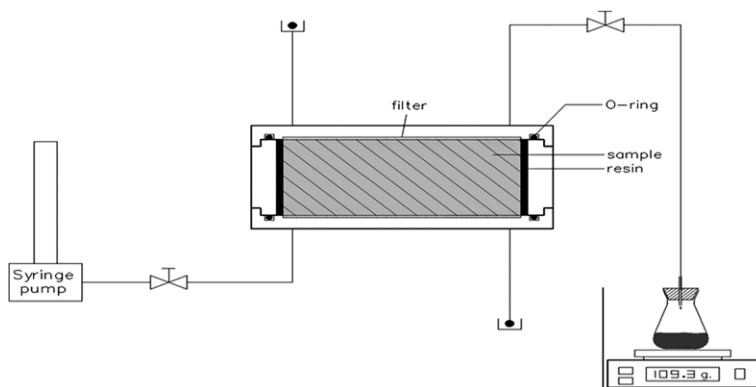


Fig. 2. Schematic of the high pressure 'constant head' experimental set-up with syringe pump.

was calculated from hydraulic conductivity using the relationship

$$k = \frac{K \eta_w}{\rho_w g} \quad (5)$$

where  $\eta_w$  is the viscosity of water ( $=0.001002$  Pa s).

### Experimental system

Independent laboratory studies were undertaken at the BGS and SCK-CEN on supplied samples of compact bentonite. Each laboratory performed a series of flow measurements using custom-designed apparatus imposing a constant volume boundary condition. These systems are described in detail below.

### Constant volume apparatus (BGS)

Figure 1 shows a schematic of the constant volume permeameter designed and commissioned specifically for this experimental study. In this geometry the specimen is volumetrically constrained, preventing dilation of the clay in any direction. The apparatus consists of four main components: (a) a thick-walled dual-closure stainless steel pressure vessel; (b) a fluid injection system; (c) a backpressure system; and (d) a data acquisition system operating within a LabView™ environment. Pressure in the injection and backpressure circuits is continuously monitored through independent pressure transducers providing a check on system pressures. Testing was performed in an air-conditioned laboratory at a nominal air temperature of around  $20 \pm 0.5$  °C.

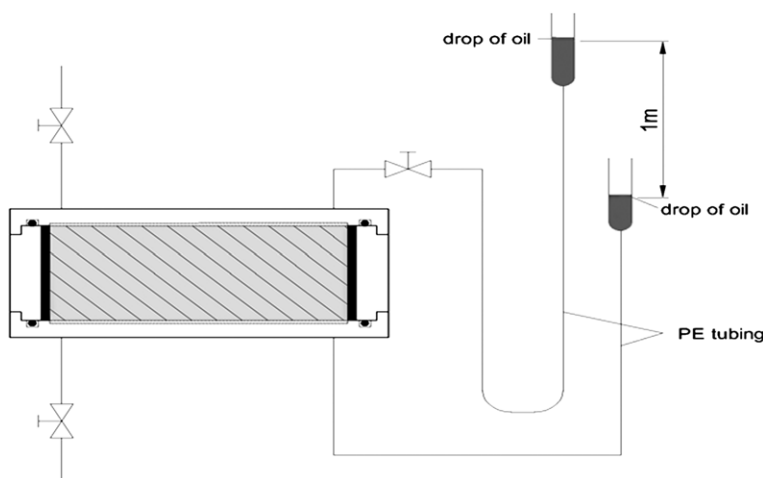
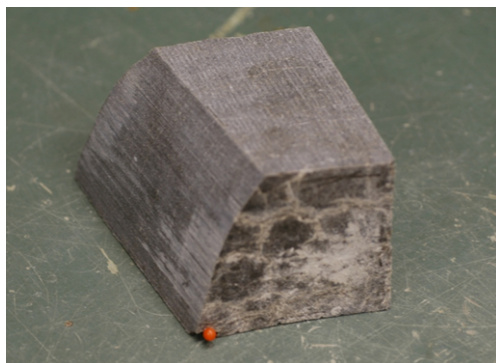


Fig. 3. Schematic of the low pressure 'constant head' experimental set-up using water columns to set the gradient.





**Fig. 5.** Photograph of a preserved sample taken from block R8, direction 300° at a distance of 540–620 mm from the centre (CRT R8:300:540). The location of the orange (online only) pin indicates the surface closest to the canister. Photograph courtesy of Clay Technology AB. Copyright SKB.

Both ISCO syringe pumps and associated pressure transducers were calibrated to a known laboratory standards, with increments and decrements in pressure to quantify hysteresis. Using a spreadsheet, least-squares regression fits were calculated and the parameters used to correct the raw data.

#### *Constant volume apparatus (SCK-CEN)*

Two experimental geometries were designed by SCK-CEN to define the hydraulic behaviour of the bentonite. Both systems were configured to perform constant head hydraulic conductivity tests in which the compact clay samples were confined within a constant volume cell, with flow in and out measured as a function of time. In this way, it is possible to specify the hydraulic gradient imposed across the sample while continuously monitoring in- and outflow until equal. Analysis of the transient phase provides an indication of the initial degree

of saturation. By measuring flux in and out of the core, it is possible to identify any leaks that might be present. The minimal hydraulic gradient at which it is possible to perform the experiment is defined by the minimal in- and outflow that can be precisely measured. An ISCO-100, Series DM, syringe pump was used to impose the inlet pressure and measure inflow, while at the outlet, no excess backpressure was imposed (i.e.  $P_{\text{out}} = \text{atmospheric pressure}$ ) as a high-precision balance used to measure outflow (Fig. 2). Both were calibrated using a high-precision balance to a known laboratory standard.

To minimize evaporation at the outlet, stainless steel tubing was used to connect the sample holder to the collection bottle, the latter closed with a septum. This allowed evaporation rates through the septum to be determined, which were found to range from 3 to 10  $\mu\text{l}/\text{week}$ . It was therefore decided to perform all measurements at an inlet pressure of around 1 MPa. Since the samples have a diameter of 50 mm and length of 50 mm (and are fully confined in the test cell), this resulted in a gradient of around 2000  $\text{m m}^{-1}$  applied to the sample. In a similar manner to BGS, test samples were machine turned on a lathe to achieve the required dimensions.

A second apparatus was constructed to try and measure the hydraulic conductivity at a much lower gradient, that is, a gradient of 20 instead of 2000. In this test system, a water column of 1.5 m in height was connected to the inlet of the sample holder and a second column of 0.5 m height connected at the outlet (Fig. 3). A drop of silicon oil was placed on the top of each column to avoid evaporation. A pipet graduated in 1  $\mu\text{l}$  intervals was then connected to both columns to provide an accurate measure of flow. Unlike the previous high-pressure apparatus (Fig. 2), connections from the sample holder to the water column were made with standard laboratory polyethylene tubing (Fig. 3).

**Table 1.** Shows the basic physical properties of all test samples prior to testing assuming a specific gravity for the mineral solids of  $2.77 \text{ mg m}^{-3}$

Sample number	Sampling interval (code)	Water content (wt%)	Bulk density ( $\text{mg m}^{-3}$ )	Dry density ( $\text{mg m}^{-3}$ )	Void ratio	Porosity	Degree of saturation (%)
CRT-1	R8:300:540	24.8	2.00	1.61	0.736	0.421	0.95 [–]
CRT-2	R8:300:850	23.5	2.05	1.66	0.67	0.400	0.98 [1.0]
CRT-3	Virgin material	27.1	1.98	1.56	0.772	0.436	0.97 [1.0]
CRT-4	R7–225-665	23.0	2.08	1.69	0.64	0.389	0.92 [1.0]
CRT-5	R7-225-765	22.2	2.09	1.71	0.621	0.383	0.90 [1.0]
CRT-6	R7-225-790	23.7	2.07	1.67	0.65	0.396	0.93 [1.0]

Inspection of the table indicates all samples started with a slight degree of desaturation ranging from 95 to 98% for ring 8 and from 90 to 93% for ring 7 (the latter measurements are based on off-cut material from the neighbouring core).

**Table 2.** Flow in and out, injection and backpressure and head gradient for each test stage of sample CRT-1 at steady-state

Sample	Step no. and stage	Flow in ( $\mu\text{l h}^{-1}$ )	Flow out ( $\mu\text{l h}^{-1}$ )	Injection pressure (MPa)	Backpressure (MPa)
CRT-1	1 (EQ)	–	–	1.00	1.00
	2 (CFR)	1.6	1.5	2.71	1.00
	3 (CFR)	2.6	2.4	3.67	1.00
	4 (CFR)	3.0	2.7	4.11	1.00
	5 (CFR)	4.6	4.3	5.83	1.00
	6 (CFR)	2.6	2.3	3.88	1.00
	7 (CFR)	1.6	1.4	2.79	1.00
CRT-2	1 (EQ)	–	–	1.00	1.00
	2 (CFR)	1.6	1.5	2.99	1.00
	3 (CFR)	2.6	2.5	4.41	1.00
	4 (CFR)	1.6	1.5	3.09	1.00
CRT-3	1 (EQ)	–	–	1.00	1.00
	2 (CFR)	1.6	1.5	2.84	1.00
	3 (CFR)	2.6	2.5	4.12	1.00
	4 (CFR)	3.0	3.0	4.67	1.00
	5 (CFR)	2.6	2.5	4.18	1.00
	6 (CFR)	1.6	1.5	2.93	1.00
	7 (CFR)	3.0	2.7	4.66	1.00
	8 (CFR)	1.6	1.5	2.94	1.00

Inspection of the data indicates a good mass balance between flow in and out with difference less than or equal to  $0.3 \mu\text{l h}^{-1}$ .

## Test material

### BGS

Testing was performed on a section of bentonite retrieved from ring 8 of the CRT (Fig. 4). Block samples of bentonite were taken in a tangential

pattern from the clay–canister interface outwards. From this material BGS selected two samples, one close to the canister surface (Fig. 5) and the other from the opposite side of the ring next to the rock wall. A third sample of ‘virgin’ clay freshly manufactured by Clay Technology AB was selected as

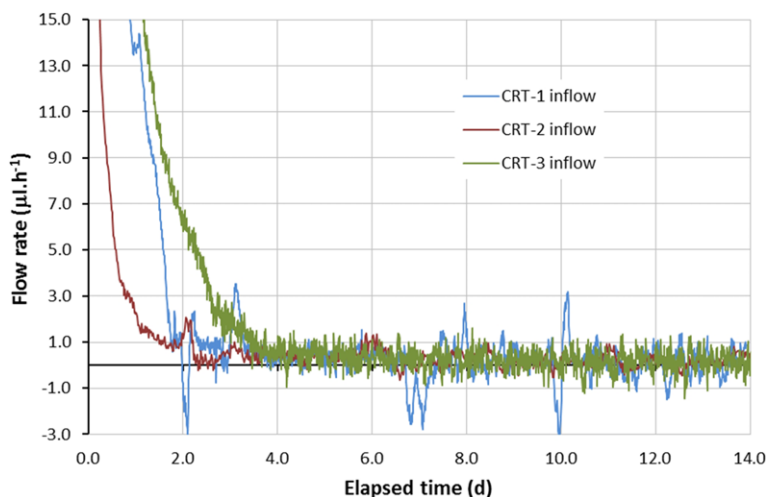


**Fig. 6.** Flow into specimens CRT-1 to -3 during the initial EQ stages (Table 2). Positive flow represent uptake of distilled water by the specimens. Inspection of the data indicates the bulk of the inflow occurs within the first 5 days which then tails off to near zero flow from 12 days onwards.

TEMPERATURE IMPACT PERMEABILITY

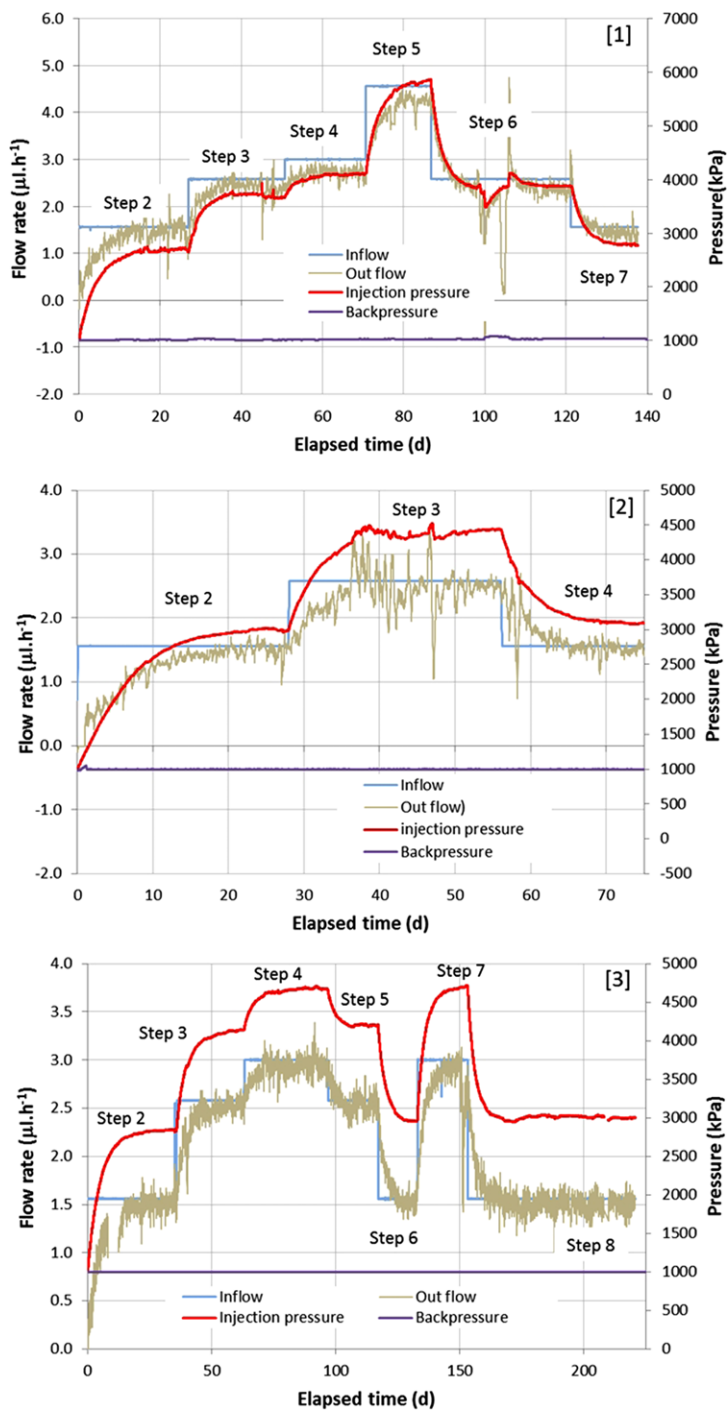


**Fig. 7.** Flow and pressure data for tests CRT-1, -2 and -3 respectively. Inspection of the data shows well-defined transients leading to steady-state conditions. Discrete spikes in data in [1] relate to small temperature fluctuations within the laboratory. Problems with the air conditioning system between 100 and 107 days resulted in a considerable noise within the data. However, projection of the flux and pressure asymptotes prior to this event suggests that it had no long term deleterious effect on the data.

**Table 3.** Hydraulic properties based on steady-state and transient analysis of the data, showing hydraulic permeability and specific storage values for each test stage

Sample no.	Stage no.	Hydraulic permeability $k$ ( $\text{m}^2 \times 10^{21}$ )		Modelled permeability $k$ ( $\text{m}^2 \times 10^{21}$ )	Modelled specific storage $S_s$ ( $\text{m}^{-1} \times 10^5$ )
		Flow in	Flow out		
CRT-1	Step 2	4.9	4.6	4.7	1.9
	Step 3	5.2	4.7	4.8	1.2
	Step 4	5.2	4.6	5.9	2.8
	Step 5	5.0	4.7	4.6	1.4
	Step 6	4.8	4.3	5.2	1.2
	Step 7	4.7	4.2	4.5	1.4
CRT-2	Step 2	4.7	4.0	4.6	1.6
	Step 3	4.5	3.9	4.3	1.1
	Step 4	4.4	3.8	4.5	1.1
CRT-3	Step 2	5.0	4.9	4.9	1.7
	Step 3	4.9	4.8	4.7	1.3
	Step 4	4.8	4.8	4.8	1.2
	Step 5	4.8	4.7	4.8	0.9
	Step 6	4.8	4.6	4.8	0.9
	Step 7	4.8	4.4	4.8	0.9
	Step 8	4.6	4.4	4.8	0.9

a control. Cylindrical test specimens with an external diameter of 60 mm were manufactured by a combination of hand-trimming using a tubular former with a sharpened leading edge (Horseman & Harrington 1994) and machine lathing (Harrington *et al.* 2012). Sample lengths were 53.9, 60.0 and 59.7 mm, respectively, for samples CRT-1, CRT-2 and CRT-3.

Table 1 shows the basic physical properties of the test specimens. Porosity and degree of saturation are based on an average grain density of  $2.77 \text{ mg m}^{-3}$ . Post-test measurements of saturation indicate the samples were fully hydrated. This is confirmed by measurements of inflow during the equilibrium (EQ) stages of each test.

### SCK-CEN

SCK-CEN received samples from ring 7 of the CRT at  $225^\circ$ . Samples were taken at 665, 765 and 790 mm radial distance. At each of these distances samples were taken, from which cylindrical cores with a diameter of 38 mm were prepared using a lathe. Samples with a length of 20 mm were prepared to measure bulk density and water content and the derived properties as given in Table 1. Samples 50 mm long were prepared for the hydraulic conductivity measurements.

## Results

### Controlled flow rate experiments (BGS)

A series of well-constrained hydraulic measurements were undertaken by BGS on three specimens

of compact bentonite. Each test comprised a series of stages (Table 2) designed to initially hydrate, equilibrate and then determine baseline hydraulic behaviour. During the initial EQ stage, the specimen is exposed to distilled water on both faces of the core, with the same pressure at either end of the sample. A constant flow rate (CFR) stage is used to evaluate permeability and involves pumping distilled water through the filter disc at low volumetric flow rates, with the same solution as the backpressuring fluid at the downstream end. Specific storage is defined by numerical modelling of the flow transients.

During each equilibrium stage the sample rapidly hydrates, exhibiting a well-defined transient leading to a near-zero flow condition after around 13 days (Fig. 6). By the end of each EQ stage, volumetric flow into the clay had reduced to an average flux of less than  $0.1 \mu\text{l h}^{-1}$ . Post-test measurements of saturation indicate that all test samples were fully hydrated.

Table 2 shows steady-state values for flow in and out of the specimens as well as injection and backpressure pressures for each stage of hydraulic testing (Fig. 7). The small discrepancy between fluxes relates to minor leakage ( $\leq 0.3 \mu\text{l h}^{-1}$ ) from one of the test systems. To accommodate this, hydraulic properties for all specimens have been calculated for both inflow and outflow data (Table 3). Transient analysis of the pressure data has been undertaken in a similar manner, yielding a second estimate for conductivity/permeability and an indication for the specific storage of the samples (Table 3, Fig. 8; Appendix 1). Examination of the conductivity data shows little variation in

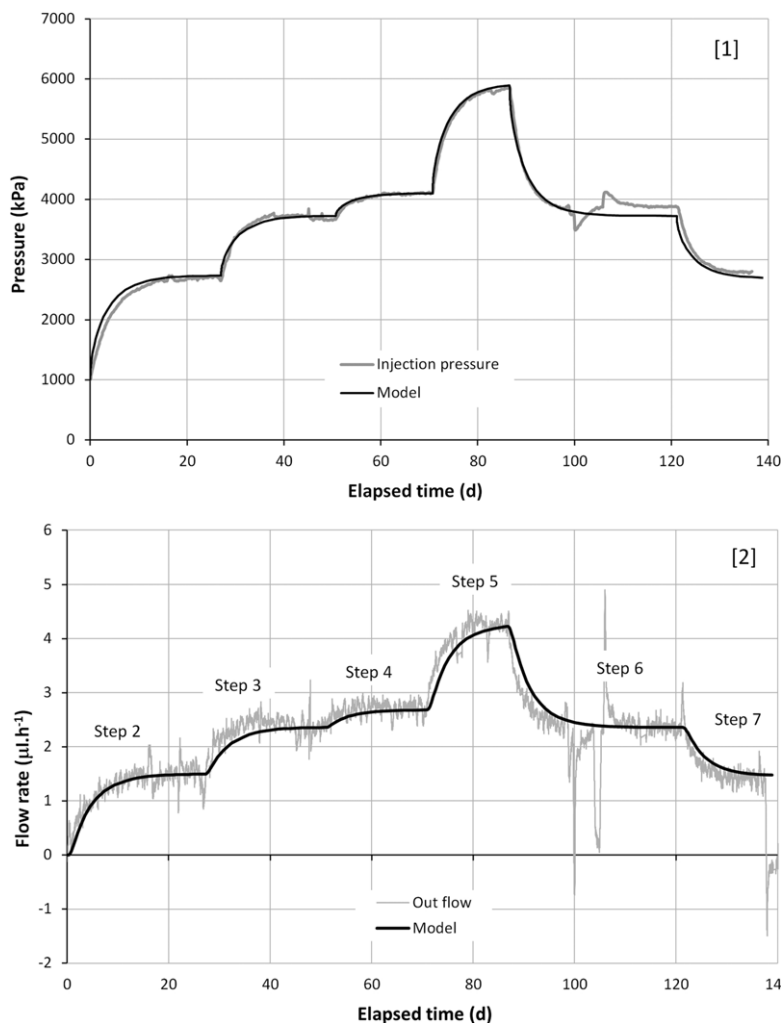


**Fig. 8.** Typical fits for hydraulic transient data (for CRT-1) based on backpressure flow rates. Plot [1] yields a good fit between predicted and measured pressures. In plot [2] there is a fairly good correlation between predicted and measured flux though some of the detail of the transients are less well-represented by the model. To improve model fits, data from test stages were individually fitted using an automated least-squares procedure optimized against the injection pressure (presented in Table 3).

values between the data processing methods, indicative of the quality of the raw data and the good mass balance obtained during hydraulic testing.

Based on analysis of the complete dataset (including analysis of the transient data), for fluxes in the range  $1.6\text{--}4.6\ \mu\text{l h}^{-1}$ , the mean hydraulic permeability is  $4.7 \times 10^{-21}\ \text{m}^2$  (standard deviation =  $0.4 \times 10^{-21}\ \text{m}^2$ ). The mean specific storage ( $S_s$ ) for the same range of flux is  $1.5 \times 10^{-5}\ \text{m}^{-1}$  (standard deviation =  $0.5 \times 10^{-5}\ \text{m}^{-1}$ ). These small standard deviations clearly demonstrate very little variation in permeability across the range of flow rates imposed. Inspection of the data

provides no evidence for the alteration of bentonite following sustained thermal exposure of up to 5 years in duration. This observation is supported by Dueck *et al.* (2010) who also noted similar results for tests on CRT material.

In these tests, head gradient was allowed to slowly evolve during each test stage as a dependent variable, simply related to the volumetric flow rate. As such, if hydraulic permeability had increased owing to thermal degradation of the buffer (Pusch *et al.* 2010), then the differential pressure for a given flow rate would scale accordingly, resulting in proportionately smaller differential pressures.

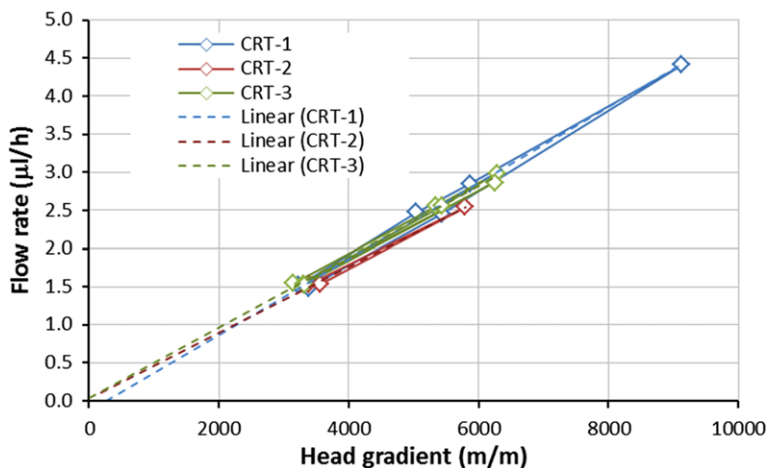


**Fig. 9.** Flow in and out of the specimens plotted against head gradient. A small amount of hysteresis in flow between advancing and decreasing cycles is observed in the data. Extrapolation of the results towards the y-axis indicates no significant threshold (i.e. non-Darcian behaviour) to flow.

A cross plot of flow rate against head gradient (Fig. 9) clearly shows that large head gradients are a necessary requirement for the movement of very small volumetric flow rates across the sample. The data exhibits only minor hysteresis between increasing and decreasing flow cycles. While controlled flow rates were varied from 1.6 to 4.6  $\mu\text{l h}^{-1}$ , values for head gradient (a dependent variable in this study) ranged from 3150  $\text{m m}^{-1}$  (at the lowest flow) to 9131  $\text{m m}^{-1}$  (at the highest). Linear regression of the data in Figure 9 yields threshold values close to zero, indicating the bentonite exhibits little if any significant threshold (i.e. non-Darcian behaviour) to hydraulic flow. This observation is supported by recent work by Villar & Gómez-Espina (2009) who undertook a series of hydraulic and hydromechanical tests for a range of clay densities at varying temperature. Their results, for clays with similar dry density, yielded only one test where flow was not detected. This observation, performed at a low hydraulic gradient, may reflect the resolution of the measurement system rather than a true threshold to flow.

#### *Constant head: controlled flow rate experiments (SCK-CEN)*

Flow data for the sample CRT-6 (R7-225-790) at 1 MPa inlet pressure are shown in Figure 10. The cumulative inflow during the first 25 days was significantly higher than afterwards. It was also significantly higher than the outflow even when taking into account the evaporation at the outlet. This clearly shows that the sample was not fully saturated at the onset of testing and that, when subject to relatively modest injection pressures of 1.0 MPa, can take 90 days or more to reach full saturation. The initial degree of saturation of the samples was found to be between 90 and 93%. This may relate to desiccation during sample preparation (drying during adjustment on the lathe) or reflect the state of saturation of the material as shipped. However, what is clear is that, owing to the resaturation of the samples in the first month, the derivation of hydraulic conductivity during this time would result in an overestimation of the fully saturated hydraulic conductivity/permeability values (Table 4). As

**Table 4.** Hydraulic properties derived from constant head experiments on samples CRT-4 to 6

Sample	Sampling interval	Conductivity ( $\text{m s}^{-1}$ )	Estimated error	Permeability ( $\text{m}^2$ )
CRT-4	R7-225-665 1	$1.3 \times 10^{-13}$	$0.8 \times 10^{-14}$	$1.3 \times 10^{-20}$
CRT-5	R7-225-765 1	$1.1 \times 10^{-13}$	$0.8 \times 10^{-14}$	$1.1 \times 10^{-20}$
CRT-4	R7-225-665 5	$4.1 \times 10^{-14}$	$0.8 \times 10^{-14}$	$4.2 \times 10^{-21}$
CRT-6	R7-225-790 5	$4.3 \times 10^{-14}$	$0.8 \times 10^{-14}$	$4.4 \times 10^{-21}$

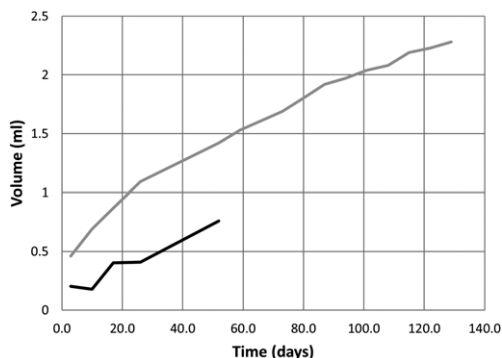


**Fig. 10.** Flow into sample CRT-6 at *c.* 1 MPa inlet pressure as function of time after initial resaturation with 1 m of water column. Grey and black lines represent cumulative in- and outflow respectively.

long as the sample is not fully saturated, the hydraulic gradient is mainly determined by the suction potential in the unsaturated bentonite sample.

#### *Low-gradient constant head tests (SCK-CEN)*

An attempt was also made to measure hydraulic conductivity at a much lower gradient, that is, 20 instead of 2000. However after 30 days it was found that the rate of evaporation through the PE tubing was around 0.2 ml/week. This value was checked by isolating the sample from the tubework and measuring the loss of fluid from the apparatus. This yielded a similar value or 0.2 ml/week, indicating that little if any flow into the clay could be detected following the initial resaturation of the clay close to the injection filter.

Importantly, if this value were to be used as the inflow parameter in the calculation the hydraulic conductivity, it would result in a gross overestimation of conductivity, yielding a value around  $10^{-19} \text{ m}^2$ . While this value would be in line with that report by Pusch *et al.* (2010), it cannot be reconciled with the data from these studies on samples of saturated compact bentonite. It should be noted that performing experiments at very low heads requires the inclusion of many precautions to avoid evaporation and temperature fluctuations. It also requires a great deal of time to get in a fully saturated state and equilibrium flow (i.e. in- and outflow equal).

## Conclusions

It has been suggested that bentonite that has been subjected to sustained thermal exposure will

exhibit a significant and permanent increase in hydraulic permeability. To examine this issue, BGS and SCK-CEN undertook a series of independent, well-constrained hydraulic measurements on a number of specimens of compact bentonite taken from the CRT performed at the Äspö Hard Rock Laboratory. To prevent bias and to ensure impartiality, the studies were conducted in isolation. Complementary approaches were adopted by each institute to measure the hydraulic properties under a range of test conditions in order to best examine potential changes in permeability.

Specific attention was paid to the choice of test technique to minimize the head gradient applied to the specimen during each test stage. In total, 19 constant flow rate tests were performed with flow rates ranging from 1.6 to  $4.6 \mu\text{l h}^{-1}$ . The duration of each test stage ranged from 14 to 64 days, with the data exhibiting well-defined transient and steady-state behaviour.

Hydraulic permeability based on both steady-state pressure and transient analysis yielded a mean value of  $4.7 \times 10^{-21} \text{ m}^2$  ( $\pm 0.4 \times 10^{-21} \text{ m}^2$ ) for fluxes in the range of  $1.6\text{--}4.6 \mu\text{l h}^{-1}$  and a mean specific storage coefficient of flux of  $1.5 \times 10^{-5} \text{ m}^{-1}$  ( $\pm 0.5 \times 10^{-5} \text{ m}^{-1}$ ). Inspection of the data clearly demonstrates no significant difference in hydraulic behaviour between the virgin material and the clay from the CRT test.

At the same time, a complimentary programme of constant pressure gradient (*c.* 1 MPa over 5 cm) tests were performed at SCK-CEN. In these experiments, saturated hydraulic permeability ranged from  $4.2$  and  $4.3 \times 10^{-21} \text{ m}^2$  with an estimated error of  $\pm 0.9 \times 10^{-21} \text{ m}^2$  owing to temperature fluctuations within the laboratory. These values are in close agreement with those derived from the BGS study.

Problems associated with low hydraulic gradient testing (owing to the prolonged restoration times and evaporation through the PE tubing) can lead to a gross overestimation of conductivity. This transient value, around  $10^{-19} \text{ m}^2$ , does not reflect the actual hydraulic properties of the bentonite when fully saturated. Under the latter conditions the permeability is clay is around  $4.4 \times 10^{-21} \text{ m}^2$ .

In contrast to values reported by Pusch *et al.* (2010), the data from this study is in close agreement with observations for unaltered saturated bentonite. It is important to note that, if the permeability of the bentonite had indeed increased by two orders of magnitude following thermal exposure, then the application of these small volumetric fluxes would have resulted in the generation of head gradients ranging from 8 to  $23 \text{ m m}^{-1}$ .

Based on these observations, the authors find no evidence for an adverse increase in hydraulic conductivity of bentonite, similar to that proposed by

Pusch *et al.* (2010), as a result of thermal exposure of the clay to temperatures of 80 °C for up to 5 years.

Funding for this study was provided by the Swedish Nuclear Fuel and Waste Management Co. (SKB). This paper is published with the permission of the Director, British Geological Survey (NERC).

## Appendix 1

Consider a specimen of length  $L_s$  and cross-sectional area  $A_s$  with hydraulic head initially everywhere at zero. A fluid flow of  $Q$  is initiated at  $t = 0$  into the specimen at the end  $x = 0$  and the response of the hydraulic head at  $x = 0$  is sought as a function of time.

The equation of one-dimensional flow is given by

$$S_s \frac{\partial h}{\partial t} = K \frac{\partial^2 h}{\partial x^2} \quad (\text{A1})$$

where  $S_s$  is the specific storage,  $K$  is the hydraulic conductivity and  $h$  is the hydraulic head. This equation must be solved subject to the boundary conditions

$$q = \frac{Q}{A_s} = -K \left. \frac{\partial h}{\partial x} \right|_{x=0} \quad (\text{A2})$$

and

$$h = 0 \quad \text{at } x = L_s \quad (\text{A3})$$

To obtain the solution to equation (A1), we take its Laplace transform,

$$pS_s \bar{h} = K \frac{\partial^2 \bar{h}}{\partial x^2} \quad (\text{A4})$$

where  $p$  is the transform parameter and  $\bar{h}$  is the Laplace Transform of the head. The solution to this may be written as

$$\bar{h}(x) = Ae^{\lambda x} + Be^{-\lambda x} \quad (\text{A5})$$

where  $A$  and  $B$  are constants to be determined from the boundary conditions and

$$\lambda = \sqrt{\frac{pS_s}{K}} \quad (\text{A6})$$

From the boundary condition in equation (A3), we have

$$Ae^{\lambda L_s} + Be^{-\lambda L_s} = 0 \quad (\text{A7})$$

Taking the Laplace transform of equation (A2), we have

$$A\lambda - B\lambda = -\left(\frac{q}{K}\right) \frac{1}{p} \quad (\text{A8})$$

Substituting using equation (A7) and re-arranging, we have

$$A = -\left(\frac{q}{K\lambda}\right) \frac{1}{p} \frac{e^{-\lambda L_s}}{e^{\lambda L_s} + e^{-\lambda L_s}} \quad (\text{A9})$$

and

$$B = \left(\frac{q}{K\lambda}\right) \frac{1}{p} \frac{e^{\lambda L_s}}{e^{\lambda L_s} + e^{-\lambda L_s}} \quad (\text{A10})$$

Thus we may write the Laplace transform of the head at  $x = 0$  as

$$\bar{h}(x=0) = \frac{q}{Kp\lambda} \tanh(\lambda L_s) \quad (\text{A11})$$

Similarly, we may write the Laplace Transform of the flow at  $x = L_s$  as

$$\bar{q}(x=L_s) = -K \left. \frac{\partial \bar{h}}{\partial x} \right|_{x=L_s} = \frac{q}{p \cosh(\lambda L_s)} \quad (\text{A12})$$

The head at  $x = 0$  and flow at  $x = L_s$  as functions of time are obtained by numerically inverting the Laplace transform solutions given in equations (A11) and (A12) using the method of Talbot (1979). Five parameters are required to define the solution. Three are experimentally determined:  $Q$ ,  $A_s$  and  $L_s$ . The remaining two are the material properties that the test is designed to determine (i.e.  $K$  and  $S_s$ ). In order to estimate the values of these parameters, a general nonlinear least squares fitting routine was used to minimize the differences between the calculated curves and the measured head data.

## References

- BRUCE, S. M., ROSENBERG, P. E. & KITTRICK, J. A. 1987. The stability of illite/smectite during diagenesis: an experimental study. *Geochimica et Cosmochimica Acta*, **51**, 2103–2115.
- DUECK, A., JOHANNESSON, L.-E., KRISTENSSON, O. & OLSSON, S. 2010. *Canister Retrieval Test at the Äspö Hard Rock Laboratory*. CRT project. Report on hydro-mechanical and chemical-mineralogical properties of the bentonite. SKB report, Stockholm.
- ENG, A. 2008. *Äspö Hard Rock Laboratory. Canister Retrieval Test. Retrieval phase*. Project report. SKB IPR-08-13, Svensk Kärnbränslehantering AB.
- FREED, R. L. & PEACOR, D. R. 1989. Variability in temperature of the smectite/illite reaction in gulf Coast sediments. *Caly Minerals*, **24**, 171–180.
- HARRINGTON, J. F., VAISSIERE, DE LA, NOY, D. J., CUSS, R. J. & TALANDIER, J. 2012. Gas flow in Callovo-Oxfordian Clay (COX): results from laboratory and field-scale. *Mineralogical Magazine*, **76**, 3303–3318.
- HORSEMAN, S. T. & HARRINGTON, J. F. 1994. *Migration of Repository Gases in an Overconsolidated Clay*. British Geological Survey, Technical report WE/94/7.
- LANSON, B., SAKHAROV, B. A., CLARET, F. & DRITS, V. A. 2009. Diagenetic smectite-to-illite transition in clay-rich sediments: a reappraisal of X-ray diffraction results using the multi-specimen method. *American Journal of Science*, **309**, 476–516.

- MEUNIER, A., VELDE, B. & DRIFFAULT, L. 1998. The reactivity of bentonites: a review. An application to clay barrier stability for nuclear waste storage. *Clay Minerals*, **33**, 9187–196.
- MOSSER-RUCK, R., CATHELINEASU, M., GUILLAUME, D., CHARPENTIER, D., ROUSSET, D., BARRES, O. & MICHAU, N. 2010. Effects of temperature, pH and iron/caly and liquid/clay ratios on experimental conversion of dioctahedral smectite to berthierine, chlorite, vermiculite, or saponite. *Clays and Clay Minerals*, **58**, 280–291.
- PUSCH, R. 1985. *Final report of the buffer mass test – volume III: chemical and physical stability of the buffer materials*. Report **85-14**. Svensk Kärnbränslehantering AB, Stockholm, Sweden.
- PUSCH, R. & WESTON, R. 2012. Superior techniques for disposal of highly radioactive waste (HLW). *Environmental Earth Science*, <http://dx.doi.org/10.1007/s12665-012-1545-y>
- PUSCH, R., KASBOHM, J. & THAO, H. T. M. 2010. Chemical stability of montmorillonite buffer clay under repository-like conditions – a synthesis of relevant experimental data. *Applied Clay Science*, **47**, 113–119.
- TALBOT, A. 1979. The accurate numerical inversion of Laplace transforms. *Journal of the Institute of Mathematics and its Applications*, **23**, 97.
- VILLAR, M. V. & GÓMEZ-ESPINA, R. 2009. Report on thermo-hydro-mechanical laboratory tests performed by CIEMAT on Febex bentonite 2004–2008. Departamento de Medio Ambiente, report no. **1178**. Conditions – a synthesis of relevant experimental data. *Applied Clay Science*, **47**, 113–119.
- VELDE, B. & VASSEUR, G. 1992. Estimation of the diagenetic smectite to illite transformation in time-temperature space. *American Mineralogist*, **77**, 967–976.
- VELDE, B., SUZUKI, T. & NICOT, E. 1986. Pressure-temperature-composition of illite/smectite mixed-layer minerals: Niger Delta mudstones and other examples. *Clays and Clay Minerals*, **34**, 435–441.